

Microwave-Tunable Diode Effect in Asymmetric SQUIDs with Topological Josephson Junctions

Joseph J. Cuzzo,^{1,*} Wei Pan,¹ Javad Shabani,² and Enrico Rossi³

¹*Materials Physics Department, Sandia National Laboratories, Livermore, CA 94551, USA.*

²*Center for Quantum Information Physics, Department of Physics, New York University, NY 10003, USA.*

³*Department of Physics, William & Mary, Williamsburg, VA 23187, USA*

In superconducting systems in which inversion and time-reversal symmetry are simultaneously broken the critical current for positive and negative current bias can be different. For superconducting systems formed by Josephson junctions (JJs) this effect is termed Josephson diode effect. In this work, we study the Josephson diode effect for a superconducting quantum interference device (SQUID) formed by a topological JJ with a 4π -periodic current-phase relationship and a topologically trivial JJ. We show how the fractional Josephson effect manifests in the Josephson diode effect with the application of a magnetic field and how tuning properties of the trivial SQUID arm can lead to diode polarity switching. We then investigate the AC response and show that the polarity of the diode effect can be tuned by varying the AC power and discuss differences between the AC diode effect of asymmetric SQUIDs with no topological JJ and SQUIDs in which one JJ is topological.

Recently there has been a great deal of activity investigating non-reciprocal effects and supercurrent rectification in superconductors^{1–16} and Josephson junctions^{17–32}. Conventional diodes, such as p-n junctions, have electrical resistance that depends on the direction of current and have numerous applications in computing, logic, and detection. The superconducting diode effect (SDE) is characterized by a difference in forward and reverse critical currents I_+ and I_- where the current range between I_+ and I_- can be used to achieve supercurrent rectification. This non-reciprocal supercurrent develops due to simultaneous breaking of time-reversal and inversion symmetry^{29,33–35}. Despite superconducting diodes having been discussed long ago^{17,36–40}, there has been a revival of interest, in part, due to signatures of finite-momentum Cooper pairing in helical superconductors^{8,26,30} associated with the Josephson diode effect (JDE). Superconducting diodes can also be used as passive on-chip gyrators, circulators, and memory in cryogenic applications⁴¹.

The fractional Josephson effect^{42,43} describes a 4π -periodic current-phase relationship in JJs originally associated with topological superconductivity. Topological superconductivity has made important strides over the past decade since theoretical proposals to create topological superconductors for use in quantum computing have become feasible to realize^{44–50}, although their discovery is still inconclusive^{51–65}. Despite this, the fractional Josephson effect is well-documented in both topological^{19,66–69} and trivial JJs⁷⁰. Furthermore, planar JJs are a suitable platform to realize a large JDE since both time-reversal and inversion symmetry can be readily and controllably broken^{71,72}.

In this article we study the DC and AC response of asymmetric SQUIDs⁷³. Compared to previous studies we take into account effects due the SQUID's inductance, the presence of an AC bias, and the role that a non-negligible fractional, 4π , component of the current-phase-relation (CPR) for one of the JJ forming SQUIDs

has on the SQUID's diode effect. We call a SQUID in which one JJ's CPR is 4π , a 2π - 4π SQUID. Recent experiments have shown that high-transparency wide JJs can also have a 4π -periodic component of the current-phase relation⁷⁰. Our approach and results do not depend on the origin of the 4π -periodic component and therefore apply directly also to SQUIDs in which one JJ is wide and very transparent, as the one studied in Ref.⁷⁰. First, we treat the problem with an analytic model that goes beyond the minimal models considered before^{72,74,75}. We show that the DC response of 2π - 4π SQUIDs exhibits the JDE and that the diode polarity is reversible with asymmetry in the normal resistance of the two SQUID arms. We compare the JDE of a topological SQUID to a topologically-trivial one and find that, despite both SQUIDs showing comparable diode efficiencies, topological SQUIDs are of higher practical quality given they have a larger rectification current window ΔI_c coinciding with large diode efficiency making them more robust to e.g. stray magnetic fields. We also show the JDE can be switched and enhanced by an AC drive allowing for a microwave-controlled diode effect. By including the inductance's effects we are able to properly characterize the ac response of the SQUID and show that the strength and sign of the diode effect depend on the ac power, an additional novel contribution toward the understanding of the physics of asymmetric SQUIDs. Lastly, we compare our analytic results with numerical simulations of the AC response of trivial asymmetric and 2π - 4π SQUIDs and find good agreement between the two approaches.

To model the dynamics of the JJs we use the resistively-shunted junction (RSJ) model: $I_B = \frac{V}{R_n} + I_s$, where a current bias I_B across a JJ is split into a resistive channel associated with quasiparticle current with normal resistance R_n and a supercurrent channel I_s . Here we ignore charging effects associated with a capacitive channel. It is known that the Coulomb energy E_C can compete with the Josephson energy E_J in a 2π - 4π SQUID and lead to a gap in the mid-gap spectrum⁷⁶ associated

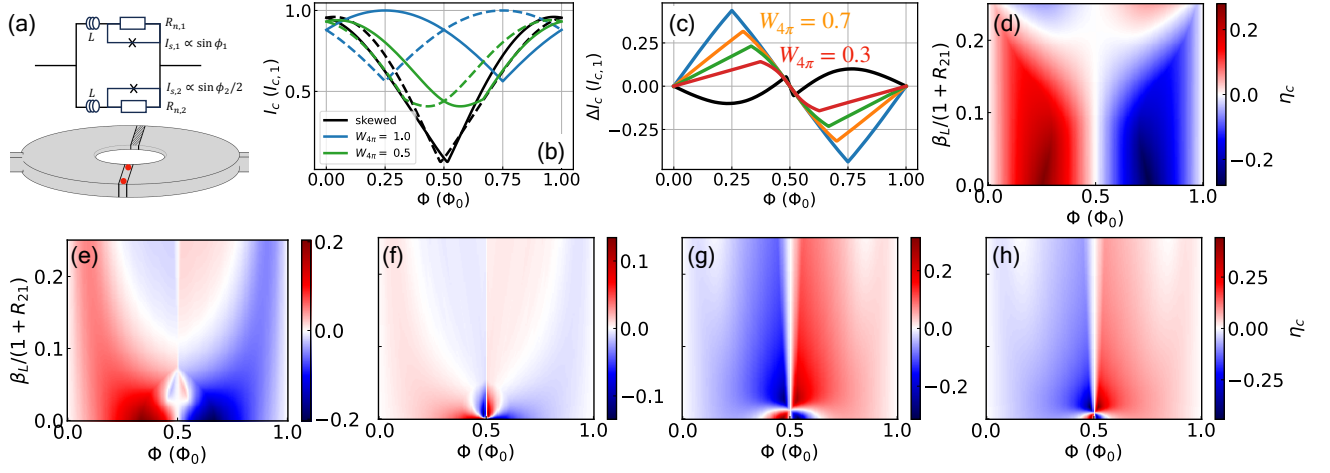


FIG. 1. (a) Circuit diagram of a 2π - 4π SQUID hosting Majorana zero modes in one arm. (b) SQUID oscillations for I_+ (solid) and I_- (dashed) with $\beta_L = 0$. Skewed SQUID parameters are $a_1 = 1$ and $a_2 = 0.9 = 1 - c_2$ and (c) corresponding critical current difference for an asymmetric SQUID with $a_1 = 1$, $b_2 = W_{4\pi} = 1 - a_2$. η_c dependence on Φ and $\frac{\beta_L}{1+R_{21}}$ for $a_1 = 1$ and (d) $W_{4\pi} = 1$, (e) $W_{4\pi} = 0.5$, (f) $W_{4\pi} = 0.1$, (g) $a_2 = 0.8$, $b_2 = 0.1 = c_2$, and (h) $a_2 = 0.9 = 1 - c_2$ (skewed SQUID).

with quantum phase slips, reducing the 4π -periodicity to 2π . Here we assume $E_J > E_C$ for both SQUID arms, corresponding to wide topological JJs^{48,77}.

We can describe the fluxoid quantization condition with s-wave superconducting electrodes for the SQUID shown in Fig. 1(a). If the superconducting electrodes are thicker than the London penetration depth and the arms have equal inductance then we have the following current conservation and flux quantization conditions: $I_B = I_1 + I_2$, $\phi_2 - \phi_1 = \frac{2\pi}{\Phi_0} \Phi_{tot} \pmod{2\pi}$ where $\Phi_{tot} = L(I_1 - I_2) + \Phi$ and $I_k = \frac{V_{J,k}}{R_{n,k}} + I_{s,k}$, $k = 1, 2$. Here I_1 and I_2 are the currents in each of the SQUID arms, ϕ_1 and ϕ_2 are the gauge-invariant phase differences across each of the SQUID arms, Φ is the total external magnetic flux through the SQUID, L is the inductance associated with the screening flux, Φ_0 denotes the superconducting magnetic flux quantum $h/2e$, and $V_{J,k}$ and $I_{s,k}$ are the potential difference and the supercurrent of the k^{th} arm, respectively. In this work, we define an asymmetric SQUID as a SQUID with at least one of the following conditions: $I_{s,1}(\phi) \neq I_{s,2}(\phi)$, $I_{c,1} \neq I_{c,2}$, or $R_{n,1} \neq R_{n,2}$. Using the Josephson relation $V_{J,k} = (\hbar/2e)\dot{\phi}_k$, we can combine these equations and solve for two coupled differential equations in terms of the average phase $\phi_A = (\phi_1 + \phi_2)/2$, and phase difference is $\Psi = (\phi_2 - \phi_1)/2\pi$

$$\frac{d\phi_A}{d\tau} = \frac{1 + R_{21}}{4} i_B - \frac{i_{s,1} + \Delta_{21} i_{s,2}}{2} + \frac{1 - R_{21}}{4\beta_L} (\Psi - \hat{\Phi}) \quad (1)$$

$$\frac{d\Psi}{d\tau} = \frac{R_{21} - 1}{4\pi} i_B + \frac{i_{s,1} - \Delta_{21} i_{s,2}}{2\pi} - \frac{1 + R_{21}}{4\pi\beta_L} (\Psi - \hat{\Phi}), \quad (2)$$

$\tau = (2\pi I_{c,1} R_{n,1} / \Phi_0) t$ is a dimensionless time, $R_{21} =$

$R_{n,2}/R_{n,1}$, $\Delta_{21} = R_{21} I_{c,2}/I_{c,1}$, $\beta_L = I_{c,1} L / \Phi_0$, $i_{s,k} = I_{s,k}/I_{c,1}$, and $\hat{\Phi} = \Phi/\Phi_0$.

Evidence for non-sinusoidal terms contributing to a skewed CPR have been observed in past experiments^{67,69,70,78–80}. To account for both the presence of skewed and topological CPRs, we assume a CPR with π -, 2π -, and 4π -periodic channels

$$i_{s,1}(\phi_1) = a_1 \sin(\phi_1) + b_1 \sin\left(\frac{\phi_1}{2}\right) + c_1 \sin(2\phi_1) \quad (3)$$

$$\Delta_{21} i_{s,2}(\phi_2) = a_2 \sin(\phi_2) + b_2 \sin\left(\frac{\phi_2}{2}\right) + c_2 \sin(2\phi_2). \quad (4)$$

The 2π periodic term of the current phase relation is standard for a JJ, the 4π -periodic contribution is present either from the topological character of the JJ or from Landau-Zener transitions in high-transparency JJs, and the π -periodic term is the leading term that needs to be included to describe JJs with good transparency. For a ballistic short junction with a mode with transmission τ , the CPR is described by $I_s(\phi) \propto \sin\phi / \sqrt{1 - \tau \sin^2(\phi/2)}$, where $0 \leq \tau \leq 1$ and ϕ is the phase across the junction. A Fourier expansion of the CPR to the second harmonic gives $I_s(\phi) \approx I_1 \sin(\phi) + I_2 \sin(2\phi)$, where $I_1 > I_2$ and I_2/I_1 depends on τ . For realistic values of τ , we have $I_2/I_1 \leq 0.1$. With this in mind, we constrain the amplitude $c_i \leq 0.1$ in our calculations. We assume $a_1 + b_1 + c_1 = 1$ and $a_2 + b_2 + c_2 = \Delta_{21}$ throughout the paper for simplicity. Furthermore, we assume $\Delta_{21} = 1$ throughout the article which implies the gaps of the junctions in the SQUID are the same. Following previous work⁸¹, we can reduce the SQUID dynamical equations to a single equation of motion by considering β_L , $|1 - R_{21}| \ll 1$. Retaining terms linear in β_L , the

SQUID dynamics are determined by the average phase ϕ_A

$$\frac{d\phi_A}{d\tau} = \frac{i_B}{2} - \tilde{i}_s(\phi_A) + \frac{\pi\beta_L(c_1 - c_2)^2}{2(1 + R_{21})} \sin(4\pi\hat{\Phi}), \quad (5)$$

where

$$\tilde{i}_s(\phi_A) = \sum_{m=1}^6 \left[x_m \sin\left(m\frac{\phi_A}{2}\right) + y_m \cos\left(m\frac{\phi_A}{2}\right) \right] + x_8 \sin(4\phi_A) + y_8 \cos(4\phi_A), \quad (6)$$

x_m and y_m are coefficients that depend on $\hat{\Phi}$, a_i , b_i , c_i , and $\beta_L/(1 + R_{21})$ ⁸². The diode efficiency $\eta_c \equiv (I_+ - I_-)/(I_+ + I_-)$ is often used to characterize superconducting diodes where the critical current I_+ ($-I_-$) corresponds to positive (negative) current bias. In an asymmetric SQUID, the broken chiral symmetry is due to different properties in the two arms of the SQUID, and the broken time-reversal symmetry is due to a magnetic flux threading the SQUID ring. For instance, in the topologically trivial asymmetric SQUID in Ref.⁷⁴, the diode is only present if an anomalous supercurrent exists at zero phase bias. This anomalous current breaks the chiral symmetry of the SQUID. We extract I_{\pm} from Eq. (5) where the last two terms describe an effective CPR. First, it is worth noting that the effect of screening enters the dynamics via the term $\beta_L/(1 + R_{21})$ suggesting an increase of R_{21} is similar to a decrease of β_L . The presence of R_{21} in the effective CPR of the SQUID can be traced back to SQUID inductance contribution to the total magnetic flux where the currents I_1 and I_2 are currents which include both the supercurrent channels *and* normal channels. Second, the last term in Eq. (5) is independent of ϕ_A but odd in $\hat{\Phi}$. This term applies an overall shift in the CPR which suggests a bipartite form of the diode effect $I_+ - I_- = \Delta\tilde{i}_{s,c} + \frac{\pi\beta_L(c_1 - c_2)^2}{2(1 + R_{21})} \sin(4\pi\hat{\Phi})$, where the former term $\Delta\tilde{i}_{s,c} = \max(\tilde{i}_s) + \min(\tilde{i}_s)$ is determined by Eq. (6) and the latter is ϕ_A -independent and associated with the screening current of imbalanced π channels. In general, a SQUID with asymmetric skewed CPRs can expect additional contributions to the screening current term, and such shifts to the CPR can contribute to anomalous scenarios such as $|\eta_c| > 1$.

We start by considering two types of SQUIDs. The first is a 2π - 4π SQUID with 4π supercurrent in the topological arm characterized by the parameter $W_{4\pi} = b_2 = 1 - a_2$. The second is a trivial asymmetric SQUID (skewed SQUID) with $a_1 = 1$ and $a_2 = 0.9 = 1 - c_2$ ($b_1 = 0 = b_2$).

The DC responses of the SQUIDs are shown in Fig. 1(b). We notice that I_c is largest when $\Phi = \Phi_0/4$ for the 2π - 4π SQUID. To understand this, recall that for a trivial SQUID with sinusoidal CPR's, the currents are maximized at $\phi_{max} = \pi/2$ and the two arms of the SQUID can simultaneously have that phase ϕ_{max} if the magnetic flux is an integer multiple of the magnetic flux quantum. Now, for the 2π - 4π SQUID, if the trivial arm has $\phi_{max,2\pi} = \pi/2$ and the non-trivial arm has

$\phi_{max,4\pi} = \pi$, then it follows from the same argument that the maximum should occur at $\Phi_{ext} = \Phi_0/4$ ^{72,83}.

In Fig. 1(c), we present the difference in critical currents $\Delta I_c = I_+ - I_-$ for the 2π - 4π SQUID and trivial asymmetric SQUID considered in Fig. 1(b). A clear Josephson diode effect develops at $\Phi \neq n\Phi_0/2$ ($n \in \mathbb{Z}$). Note, ΔI_c of the 2π - 4π SQUID exceeds that of the trivial asymmetric SQUID until $W_{4\pi} < 0.3$.

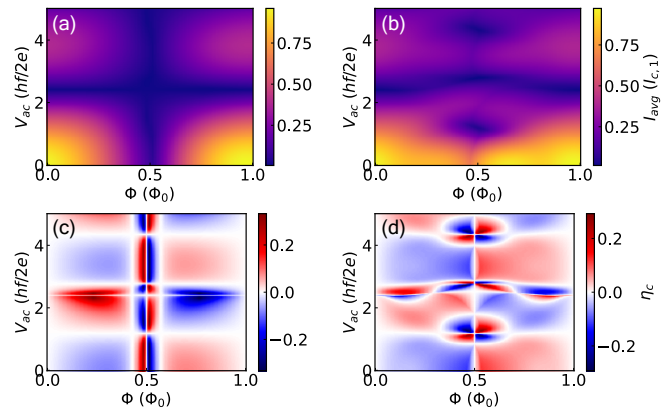


FIG. 2. AC power dependence of I_c and η_c for the skewed SQUID with (a,c) $\frac{\beta_L}{1+R_{21}} = 0$ and (b,d) $\frac{\beta_L}{1+R_{21}} = 0.125$.

We present η_c dependence on Φ and screening $\beta_L/(1 + R_{21})$ for 2π - 4π SQUIDs in Fig. 1(d-f). The diode efficiency of the 2π - 4π SQUID shown in Fig. 1(d) shows extrema for $\beta_L/(1 + R_{21}) = 0$ and diode polarity switching for large screening. As $W_{4\pi}$ is decreased from unity (panels (e-f)), η_c varies but the tunability of the diode polarity persists. Furthermore, as $W_{4\pi}$ decreases, the diode efficiency is generally smaller.

For a SQUID nearly saturated with trivial supercurrent ($a_1 = 1$, $a_2 = 0.8$, and $b_2 = c_2 = 0.1$), the regime of polarity switching with β_L is pushed beyond our approximation of $\beta_L \ll 1$ (Fig. 1(g)) and closely resembles the trivial asymmetric SQUID DC response (Fig. 1(h)). In the case of a trivial symmetric SQUID where $a_1 = 1 = a_2$, the diode efficiency $\eta_c = 0$ regardless of the value of Φ and R_{21} ⁷⁴; this also holds for $\beta_L > 0$. The source of the diode polarity switching with $\beta_L/(1 + R_{21})$ is higher harmonic contributions to the CPR associated with the screening current ($\beta_L > 0$). The inclusion of β_L and R_{21} is one of our main analytic results. We also see that η_c of the trivial asymmetric SQUID can be larger than η_c of the 2π - 4π SQUID. The reason for this is that η_c approaches unity when one of the critical currents approaches zero. Typically, this indicates an ideal diode, but if the non-zero critical current is also extremely small the practicality of such a diode is diminished since the current window for supercurrent rectification is also small. Using $|\Delta I_c|$ as an additional quality-factor we find that the 2π - 4π SQUID diode outperforms the trivial asymmetric SQUID (See Appendix D and Fig. 6). The smallness of I_c at half-flux is also the reason for the presence of strong variations, and polarity switchings, of η_c when $\Phi/\Phi_0 \approx 1/2$. Such

variations are physically uninteresting. In the remainder when discussing polarity switchings of η_c we refer to switchings at values of Φ/Φ_0 away from $1/2$. We discuss η_c in the remainder of the Letter for simplicity and comparison with the available literature, but we caution an over-emphasis on optimizing η_c without consideration of the operational current range ΔI_c . Our results also suggest the control of the diode polarity with R_{21} could be used as a signature of the fractional Josephson effect.

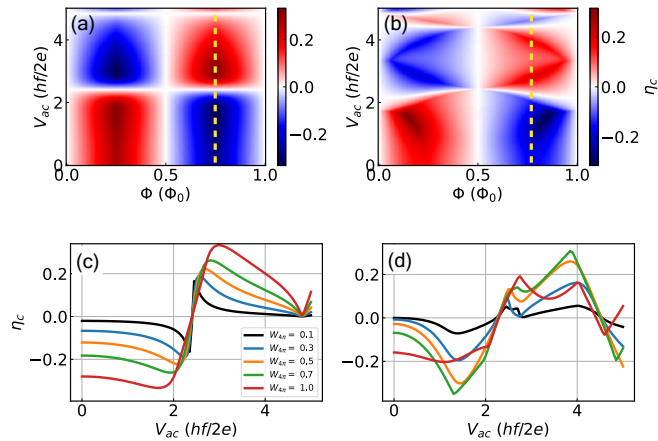


FIG. 3. AC power dependence of η_c for a 2π - 4π SQUID with (a) $\beta_L = 0$ and (b) $\beta_L/(1 + R_{21}) = 0.125$. η_c versus V_{ac} at $\hat{\Phi} = 3/4$ for $a_1 = 1$ with (c) $\beta_L = 0$ and (d) $\beta_L/(1 + R_{21}) = 0.125$.

To study the AC response of asymmetric SQUIDs we first consider the voltage-biased case, since in this regime we can obtain analytical results. Assuming $V(t) = V_{dc} + V_{ac} \cos(2\pi ft)$, from the Josephson relation $\hbar d\phi_A/dt = 2eV$, we obtain $\phi_A(t) = \phi_0 + \omega_0 t + z \sin(2\pi ft)$ where ϕ_0 is an arbitrary integration constant, $z = 2eV_{ac}/(\hbar f)$, and $\omega_0 = 2eV_{dc}/\hbar$. Using Eqs. (5-6) we can obtain the $\bar{I} - V_{dc}$, with \bar{I} being the time-averaged current, characteristic of the SQUID. In the remainder we focus on the the behavior of the current when $V_{dc} = 0$.

Figures 2(a-b) show the SQUID critical current $I_{avg} \equiv I_+ + I_-$ as a function of Φ and V_{ac} for $\beta_L/(1 + R_{21}) = 0$ and 0.125 , respectively, for the skewed SQUID. In the absence of screening, I_{avg} has a high degree of symmetry in (Φ, V_{ac}) space defined by lines of $I_{avg} = 0$ at $\Phi = \Phi_0/2$ and $V_{ac} \sim 2.5 \hbar f/2e$. With screening, lines of $I_{avg} = 0$ become broken and distorted. To see how this translates to the JDE, we present the corresponding diode efficiency in Fig. 2(c-d). We immediately notice the symmetry of I_{avg} is preserved in η_c , particularly where $I_{avg} \sim 0$. In fact, η_c has extrema near $I_{avg} \sim 0$ as a consequence of $I_{\pm} \rightarrow 0$ and $I_{\mp} > 0$, as discussed earlier. We observe periodic diode polarity switching with increasing microwave power V_{ac} for fixed Φ .

We can compare the AC response of the skewed SQUID of Fig. 2 with a 2π - 4π SQUID shown in Fig. 3. Panel (a) and (b) show the AC response for $\beta_L/(1 + R_{21}) = 0$ and 0.125 , respectively. We notice the extrema of η_c

occur further away from $\Phi = \Phi_0/2$ compared to a trivial asymmetric SQUID, and the magnitude of V_{ac} required to flip the diode polarity is generally larger than that of a trivial SQUID by a factor of two. The change in diode polarity can be attributed to the $J_0(z/2)$ Bessel function contribution to the gap, associated with the 4π channel, which evolves with z more slowly than the trivial Bessel dependence. Similar to a trivial asymmetric SQUID, a screening current distorts the symmetry of $\eta_c(\Phi, V_{ac})$.

In Fig. 4, we consider the influence of microwave power in the experimentally-relevant current bias regime. We numerically solve the coupled system of non-linear differential equations described in Eq. (2) where we are not limited by the approximation β_L , $|1 - R_{21}| \ll 1$ used thus far. We consider a current bias $I_B = I_{dc} + I_{ac} \cos(2\pi ft)$ with a driving frequency $\hbar f/\pi\Delta = 0.6$ where $\pi\Delta \equiv 2eI_c R_n$ ⁸⁴.

Fig. 4(a) shows the power dependence of the dV/dI characteristics for a trivial asymmetric SQUID ($\Phi = \Phi_0/4$) where the diode polarity gradually switches at high powers, as shown in panel (b). Dashed lines indicate a diode polarity switch. In agreement with Fig. 2(c-d), η_c has a soft sign switch at low power before switching abruptly as the critical currents are nearly suppressed. Also in agreement with Fig. 2(c-d), η_c has extrema as the critical currents are suppressed. Figure 4(c-d) presents the microwave response of a 2π - 4π SQUID. We note that the polarity of the 2π - 4π SQUID is opposite to that of the trivial asymmetric SQUID at zero AC power. η_c has a weak enhancement in magnitude at lower I_{ac} before a gradual sign change at $I_{ac} = I_c$, which is at a higher power the first polarity switch of the asymmetric SQUID ($I_{ac} \sim 0.6I_c$). Generally, the numerical results indicate good agreement with the analytic calculations. The dV/dI characteristics are generally non-reciprocal, showing different Shapiro steps for positive and negative I_{dc} ⁷⁵.

In this article, we studied the JDE in the DC and AC response of asymmetric SQUIDs, including the effects of inductance and asymmetries in I_c and R_n . We showed that the inductance β_L and the ratio $R_{21} = R_{n,2}/R_{n,1}$ can tune the diode efficiency of an asymmetric DC SQUID. Such results may be applicable to recent experimental demonstrations of gate-tunable diode effects in asymmetric SQUIDs^{85,86}. For SQUIDs with a 4π junction, tuning β_L and R_{21} can cause a switching on the diode polarity. We also showed a 2π - 4π SQUID has the opposite diode polarity of a trivial SQUID over a wide range of $\beta_L/(1 + R_{21})$ and $\hat{\Phi}$. We then discussed how the Josephson diode polarity and efficiency of asymmetric SQUIDs can be controlled by microwave irradiation. We presented calculations of the AC response of asymmetric SQUIDs where the diode efficiency and polarity are controlled by the AC power. The advantage of probing non-reciprocal transport in the AC response is that missing Shapiro steps indicative of a fractional Josephson effect have been observed experimentally^{19,66-70}, suggesting the AC response of a 2π - 4π SQUID can readily be

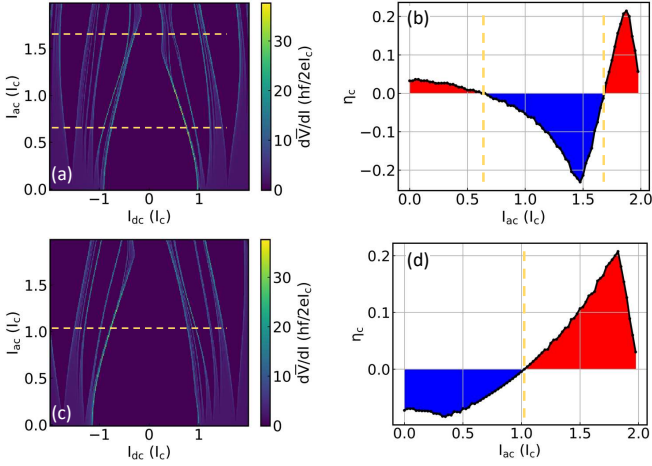


FIG. 4. SQUID microwave response under current bias with $\hat{\Phi} = 3/4$ and $\beta_L = 1$ for (a-b) the skewed SQUID with $a_1 = 1$, $a_2 = 0.9 = 1 - c_2$, $R_{21} = 2$ and (c-d) 2π - 4π . Dashed lines indicate powers at which $\eta_c = 0$.

observed regardless of whether the 4π junction is topological or not.

ACKNOWLEDGMENTS

W.P., J.S., and E.R. acknowledge support from DOE, Grant No DE-SC0022245. The work at Sandia is supported by a LDRD project. Sandia National Laboratories is a multimission laboratory managed and operated by National Technology and Engineering Solutions of Sandia LLC, a wholly owned subsidiary of Honeywell International Inc. for the U.S. DOE's National Nuclear Security Administration under contract DE-NA0003525. This paper describes objective technical results and analysis. Any subjective views or opinions that might be expressed in the paper do not necessarily represent the views of the U.S. DOE or the United States Government.

Appendix A: 2π - 4π SQUID dynamics

We start with the model for a semiclassical description of SQUID dynamics:

$$I_{bias} = I_1 + I_2 \quad (A1)$$

$$\phi_2 - \phi_1 = \frac{2\pi}{\Phi_0} \Phi_{tot} \quad (A2)$$

$$\Phi_{tot} = L(I_1 - I_2) + \Phi \quad (A3)$$

$$I_i = \frac{V_{J,i}}{R} + I_{s,i} + C_i \frac{dV_{J,i}}{dt} \quad (A4)$$

where I_1 and I_2 are the currents in each of the SQUID arms, ϕ_1 and ϕ_2 are the gauge-invariant phase differences across the JJ's in each of the SQUID arms, Φ is the total external magnetic flux through the SQUID, L is the

inductance associated with the screening flux, and $V_{J,i}$ and $I_{s,i}$ for $i = 1, 2$ are the potential difference across the i^{th} JJ and the pair current in the i^{th} JJ, respectively. We can consider the general RCSJ model for a SQUID device,

$$\frac{d^2\phi_1}{d\tau'^2} + \sigma \frac{d\phi_1}{d\tau'} = \frac{i_B}{2} - i_{s,1}(\phi_1) + \frac{1}{4\pi\beta_L} (\phi_2 - \phi_1 - 2\pi\hat{\Phi}) \quad (A5a)$$

$$C_{21} \frac{d^2\phi_2}{d\tau'^2} + \frac{\sigma}{R_{21}} \frac{d\phi_2}{d\tau'} = \frac{i_B}{2} - I_{21} i_{s,2}(\phi_2) - \frac{1}{4\pi\beta_L} (\phi_2 - \phi_1 - 2\pi\hat{\Phi}) \quad (A5b)$$

where $C_{21} = C_2/C_1$, $I_{21} = I_{c,2}/I_{c,1}$, $R_{21} = R_{n,2}/R_{n,1}$, $\sigma = \sqrt{\Phi_0/2\pi I_{c,1} R_{n,1}^2 C_1}$ and $\tau' = \sqrt{2\pi I_{c,1}/\Phi_0 C_1} t$. We will work in the overdamped regime for simplicity, but the extension is straightforward. Numerical calculations are generated by solving the system of coupled differential equations in the overdamped regime where capacitance is neglected.

For a 2π - 4π SQUID, we consider the supercurrents $i_{s,1} = \sin(\phi_1)$ and $i_{s,2} = \sin(\phi_2/2)$ where $R_{21} = I_{21} = 1$. We can reduce the SQUID dynamical equations to a single dynamical equation as a function of the average phase across the SQUID $\phi_A = (\phi_1 + \phi_2)/2$ by considering the inductance β_L to be perturbatively small⁸¹. The resulting dynamical equation is $i_B/2 = \frac{d\phi_A}{d\tau} + \tilde{i}_s(\phi_A, \hat{\Phi}_{ext})$ where $\tau \equiv (2\pi R I_{2\pi}/\Phi_0) t$ and,

$$\begin{aligned} \tilde{i}_s(\phi_A, \hat{\Phi}) &= \frac{1}{2} \sin\left(\frac{\phi_A + \pi\hat{\Phi}}{2}\right) + \frac{1}{2} \sin(\phi_A - \pi\hat{\Phi}) \\ &- \frac{\pi\beta_L}{8} \left[2 \sin(2(\phi_A - \pi\hat{\Phi})) + \sin(\phi_A + \pi\hat{\Phi}) \right] \\ &- \frac{\pi\beta_L}{8} \left[\sin\left(\frac{\phi_A - 3\pi\hat{\Phi}}{2}\right) - 3 \sin\left(\frac{3\phi_A - \pi\hat{\Phi}}{2}\right) \right]. \end{aligned} \quad (A6)$$

1. DC Response

We find that the SQUID dc response to magnetic flux in the 2π - 4π SQUID is asymmetric: $I_{max}(\hat{\Phi}, I_{dc}) \neq I_{max}(-\hat{\Phi}, I_{dc}) \neq I_{max}(\hat{\Phi}, -I_{dc})$. The symmetry retained in the system is $I_{max}(\hat{\Phi}, I_{dc}) = I_{max}(-\hat{\Phi}, -I_{dc})$.

Besides this general asymmetry, we also notice that the maximum critical current does not manifest at $\Phi = 0$. Recall that for a trivial SQUID with sinusoidal CPR's, the currents are maximized at $\phi_{max} = \pi/2$ and the two arms of the SQUID can simultaneously have that phase ϕ_{max} if the magnetic flux is an integer multiple of the

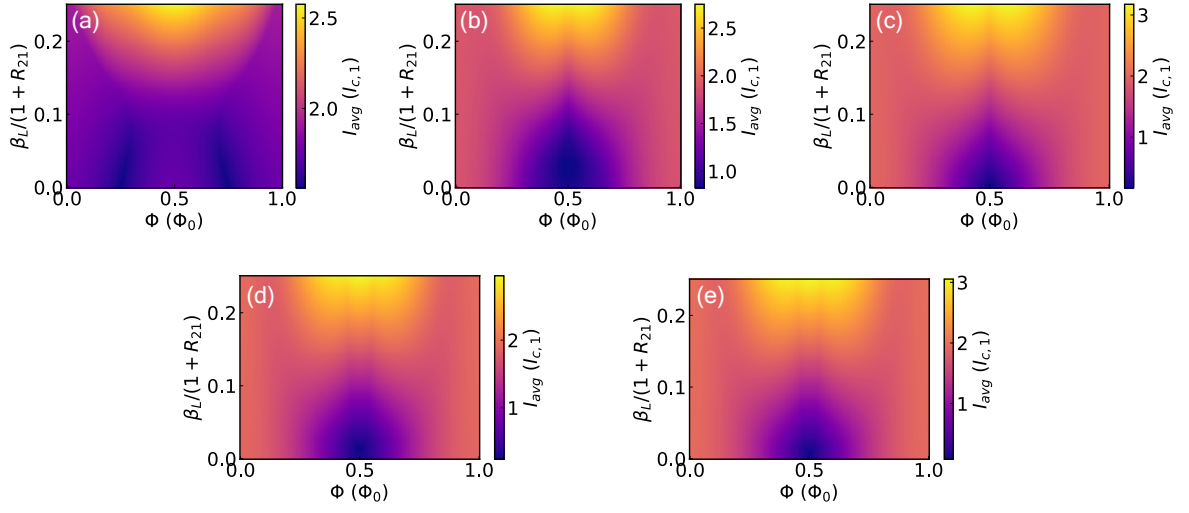


FIG. 5. I_{avg} dependence on Φ and $\frac{\beta_L}{1+R_{21}}$ for $a_1 = 1$ and (a-c) various values of $W_{4\pi}$, (e) $a_2 = 0.8$, $b_2 = 0.1 = c_2$, and (f) $a_2 = 0.9 = 1 - c_2$ (trivial SQUID).

magnetic flux quantum:

$$\phi_2 - \phi_1 = \frac{2\pi\Phi}{\Phi_0} \pmod{2\pi} \quad (\text{A7})$$

Now, for the 2π - 4π SQUID, if the trivial arm (say, arm 1) has $\phi_{max,1} = \pi/2$ and the non-trivial arm has $\phi_{max,2} = \pi$, then it follows from the argument for the trivial SQUID that the maximum should occur at $\Phi = \Phi_0/4$.

Appendix B: Symmetric SQUID with π -, 2π -, & 4π -periodic Channels

In this section, we provide the general solution for a symmetric DC SQUID circuit model with negligible capacitance, weak inductance, and a supercurrent with π -, 2π -, and 4π -periodic channels. We write an effective description of the supercurrent channel with a skewed CPR and a topological contribution as,

$$I_s = I_{4\pi} \sin(\phi/2) + I_{2\pi} \sin(\phi) + I_\pi \sin(2\phi). \quad (\text{B1})$$

Making use of the ac Josephson effect $\frac{d\phi}{dt} = \frac{2e}{\hbar} V$, we find

$$\frac{d\phi_1}{d\tau} + \sin(\phi_1) + \tilde{\beta} \sin(2\phi_1) + \alpha \sin(\phi_1/2) + \frac{\phi_1 - \phi_2}{4\pi\beta_L} = \frac{1}{2} \left(i_B - \frac{\hat{\Phi}}{\beta_L} \right) \quad (\text{B2})$$

$$\frac{d\phi_2}{d\tau} + \sin(\phi_2) + \tilde{\beta} \sin(2\phi_2) + \alpha \sin(\phi_2/2) - \frac{\phi_1 - \phi_2}{4\pi\beta_L} = \frac{1}{2} \left(i_B + \frac{\hat{\Phi}}{\beta_L} \right) \quad (\text{B3})$$

where $\tilde{\beta} \equiv I_\pi/I_{2\pi}$, $\alpha \equiv I_{4\pi}/I_{2\pi}$, $\beta_L \equiv LI_{2\pi}/\Phi_0$,

$i_B \equiv I_{bias}/I_{2\pi}$, $\hat{\Phi} \equiv \Phi/\Phi_0$, and $\tau \equiv (2\pi R_{n,1} I_{2\pi}/\Phi_0)t$. Defining $\phi_A \equiv (\phi_1 + \phi_2)/2$ and $\Psi \equiv (\phi_2 - \phi_1)/2\pi$, we can consider the sum and difference of equations to find

$$\frac{d\phi_A}{d\tau} + \sin(\phi_A) \cos(\pi\Psi) + \tilde{\beta} \sin(2\phi_A) \cos(2\pi\Psi) + \alpha \sin(\phi_A/2) \cos(\pi\Psi/2) = \frac{i_B}{2} \quad (\text{B4})$$

$$\pi \frac{d\Psi}{d\tau} + \frac{\Psi}{2\beta_L} + \sin(\pi\Psi) \cos(\phi_A) + \tilde{\beta} \sin(2\pi\Psi) \cos(2\phi_A) + \alpha \sin(\pi\Psi/2) \cos(\phi_A/2) = \frac{\hat{\Phi}}{2\beta_L} \quad (\text{B5})$$

Assuming $\beta_L \ll 1$, we make the following ansatz:

$$\Psi(\tau) = \hat{\Phi} + \beta_L \Psi_1(\tau) + \mathcal{O}(\beta_L^2) \quad (\text{B6})$$

Substituting, we find the solution to lowest order in β_L

is

$$\begin{aligned} \Psi_1(\tau) = & -2[\alpha \sin(\pi\hat{\Phi}/2) \cos(\phi_A/2) \\ & + \tilde{\beta} \sin(2\pi\hat{\Phi}) \cos(2\phi_A) + \sin(\pi\hat{\Phi}) \cos(\phi_A)]. \quad (\text{B7}) \end{aligned}$$

Now we can reduce the system of coupled equations into a single equation for ϕ_A and calculate the time-averaged current bias for an rf-driven junction. Substituting Eq. B7 into Eq. B4 and simplifying, we find

$$\begin{aligned} \frac{d\phi_A}{d\tau} + a \sin(\phi_A) + b \sin(2\phi_A) + c \sin(3\phi_A) + d \sin(4\phi_A) \\ + f \sin\left(\frac{\phi_A}{2}\right) + g \sin\left(\frac{3\phi_A}{2}\right) + h \sin\left(\frac{5\phi_A}{2}\right) = \frac{i_B}{2} \quad (\text{B8}) \end{aligned}$$

for the coefficients,

$$a = x(1 - \pi\beta_L\tilde{\beta}y^2) + \frac{\pi}{4}\alpha^2\beta_L(1 - x) \quad (\text{B9})$$

$$b = \tilde{\beta} + (\pi\beta_L - 2\tilde{\beta})y^2 \quad (\text{B10})$$

$$c = 6\pi\beta_L\tilde{\beta}xy^2 \quad (\text{B11})$$

$$d = 2\pi\beta_L\tilde{\beta}^2y^2 \quad (\text{B12})$$

$$f = \alpha(C_{\pi/2} + \frac{\pi}{2}\beta_LyS_{\pi/2}) \quad (\text{B13})$$

$$g = \frac{3\pi}{2}\alpha\beta_Ly(1 + 2\tilde{\beta}x)S_{\pi/2} \quad (\text{B14})$$

$$h = 5\pi\alpha\beta_L\tilde{\beta}xyS_{\pi/2} \quad (\text{B15})$$

where $S_{\pi/2} \equiv \sin(\pi\hat{\Phi}/2)$, $C_{\pi/2} \equiv \cos(\pi\hat{\Phi}/2)$, $x \equiv \cos(\pi\hat{\Phi})$, and $y \equiv \sin(\pi\hat{\Phi})$. Note that if $\hat{\Phi} = 0$, then only a , b and f are non-zero. The coefficients in Eq. (B8) have the following interpretations:

- a : 2π channel of each arm, the *interference* of the 4π channels of the arms, and *interference* of the 2π and π channels of the arms
- b : π channel of each arm and the *interference* of the 2π channels of the arms

- c : *interference* of the 2π and π channels of the arms
- d : *interference* of the π channels of the arms
- f : 4π channel of each arm
- g : *interference* of 4π and 2π channels of the arms, and the *interference* of 4π and π channels of the arms
- h : *interference* of 4π and π channels of the arms

1. Voltage-bias solution

From here, we can consider a voltage bias

$$V(\tau) = V_0 + V_1 \cos(\omega\tau) \quad (\text{B16})$$

and make use of the ac Josephson effect

$$\frac{d\phi_A}{dt} = \frac{2e}{\hbar}V$$

to solve for $\phi_A(\tau)$ and substitute into Eq. B8. Then we can use the Jacobi-Anger expansion,

$$e^{iz \sin(\theta)} = \sum_{n=-\infty}^{+\infty} J_n(z) e^{in\theta}, \quad (\text{B17})$$

where J_n are n^{th} order Bessel functions, to calculate the Shapiro spikes and each spike's width.

Now we will describe how to calculate Shapiro spike widths in terms of the time-averaged pair current \bar{I}_s and specifically consider the $n = 0$ spike. We start by integrating the ac Josephson effect from the end of the previous section. We can write (in dimensionless parameters),

$$\phi_A(\tau) = \phi_0 + \omega_0\tau + z \sin(\omega\tau) \quad (\text{B18})$$

where ϕ_0 is an arbitrary integration constant, $z = 2eV_1/\hbar\omega$, and $\omega_0 = 2eV_0/\hbar$. We then substitute into Eq. (B8) to get $2d\phi_A/d\tau + I_s = i_B$ where

$$\begin{aligned} I_s = 2\text{Im}\{ \sum_{n=-\infty}^{+\infty} (-1)^n e^{-in\omega\tau} [a e^{i(\phi_0 + \omega_0\tau)} J_n(z) + b e^{2i(\phi_0 + \omega_0\tau)} J_n(2z) + c e^{3i(\phi_0 + \omega_0\tau)} J_n(3z) \\ + d e^{4i(\phi_0 + \omega_0\tau)} J_n(4z) + f e^{\frac{1}{2}i(\phi_0 + \omega_0\tau)} J_n(z/2) + g e^{\frac{3}{2}i(\phi_0 + \omega_0\tau)} J_n(3z/2) + h e^{\frac{5}{2}i(\phi_0 + \omega_0\tau)} J_n(5z/2)] \} \quad (\text{B19}) \end{aligned}$$

Appendix C: Asymmetric SQUID dynamics

Now we assume a general CPR with π -, 2π -, and 4π -periodic channels,

$$i_{s,1}(\phi_1) = a_1 \sin(\phi_1) + b_1 \sin\left(\frac{\phi_1}{2}\right) + c_1 \sin(2\phi_1) \quad (\text{C1})$$

$$\Delta_{21} i_{s,2}(\phi_2) = a_2 \sin(\phi_2) + b_2 \sin(\phi_2/2) + c_2 \sin(2\phi_2) \quad (\text{C2})$$

where $\Delta_{21} = I_{c,2}R_{n,2}/I_{c,1}R_{n,1}$. If we assume β_L , $|1 - R_{21}| \ll 1$ then we can reduce the system of 2 ODE's to a single ODE via perturbative ansatz similar to the ansatz

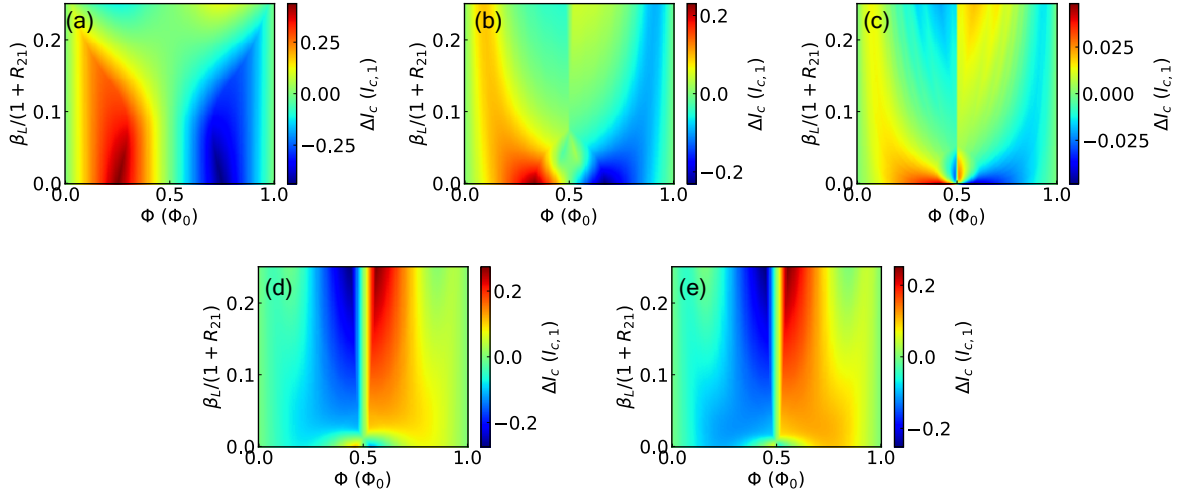


FIG. 6. ΔI_c dependence on Φ and $\frac{\beta_L}{1+R_{21}}$ for $a_1 = 1$ and (a-c) various values of $W_{4\pi}$, (e) $a_2 = 0.8$, $b_2 = 0.1 = c_2$, and (f) $a_2 = 0.9 = 1 - c_2$ (trivial SQUID).

made by de Luca:

$$\frac{d\phi_A}{d\tau} = \frac{i_B}{2} - \tilde{i}_s(\phi_A) + \frac{\pi\beta_L(c_1 - c_2)^2}{2(1 + R_{21})} S_4 \quad (\text{C3})$$

where

$$\begin{aligned} \tilde{i}_s(\phi_A) = & x_2 \sin(\phi_A) + x_4 \sin(2\phi_A) + x_6 \sin(3\phi_A) + x_8 \sin(4\phi_A) + x_1 \sin(\phi_A/2) + x_3 \sin(3\phi_A/2) + x_5 \sin(5\phi_A/2) \\ & + y_2 \cos(\phi_A) + y_4 \cos(2\phi_A) + y_6 \cos(3\phi_A) + y_8 \cos(4\phi_A) + y_1 \cos(\phi_A/2) + y_3 \cos(3\phi_A/2) + y_5 \cos(5\phi_A/2). \end{aligned} \quad (\text{C4})$$

The coefficients of the effective supercurrent \tilde{i}_s are ($C_n \equiv \cos(n\pi\hat{\Phi})$ and $S_n \equiv \sin(n\pi\hat{\Phi})$):

$$x_2 = \frac{\pi\beta_L b_1 b_2}{2(1 + R_{21})} + \left[\frac{a_1 + a_2}{2} - \frac{\pi\beta_L}{1 + R_{21}} \left(\frac{b_1^2}{2} - a_1 c_1 + a_1 c_2 + \frac{b_2^2}{4} - \frac{a_2 c_1}{2} \right) \right] C_1 - \frac{\pi\beta_L}{1 + R_{21}} \left(a_2 c_1 - \frac{a_2 c_2}{2} + \frac{a_1 c_1}{2} \right) C_3 \quad (\text{C5})$$

$$y_2 = \left[\frac{a_2 - a_1}{2} - \frac{\pi\beta_L}{1 + R_{21}} \left(a_1 c_1 - \frac{a_1 c_2}{2} + \frac{b_2^2}{4} - \frac{a_2 c_1}{2} \right) \right] S_1 - \frac{\pi\beta_L}{1 + R_{21}} \left(\frac{a_2 c_2}{2} - a_2 c_1 + \frac{a_1 c_1}{2} \right) S_3 \quad (\text{C6})$$

$$x_4 = \frac{\pi\beta_L a_1 a_2}{1 + R_{21}} + \left(\frac{c_1 + c_2}{2} - \frac{\pi\beta_L(a_1^2 + a_2^2)}{2(1 + R_{21})} \right) C_2 \quad (\text{C7})$$

$$y_4 = \left(\frac{c_2 - c_1}{2} - \frac{\pi\beta_L(a_2^2 - a_1^2)}{4(1 + R_{21})} \right) S_2 \quad (\text{C8})$$

$$x_6 = -\frac{\pi\beta_L}{1 + R_{21}} \left(\frac{a_2 c_2}{2} - 2a_2 c_1 - \frac{a_1 c_1}{2} - a_1 c_2 \right) C_1 - \frac{\pi\beta_L}{1 + R_{21}} \left(2a_1 c_1 + \frac{a_2 c_1}{2} + a_2 c_2 + \frac{a_1 c_2}{2} \right) C_3 \quad (\text{C9})$$

$$y_6 = -\frac{\pi\beta_L}{1 + R_{21}} \left(2a_2 c_1 - \frac{a_2 c_2 + a_1 c_1}{2} - a_1 c_2 \right) S_1 - \frac{\pi\beta_L}{1 + R_{21}} \left(-2a_1 c_1 + \frac{a_2 c_1}{2} + a_2 c_2 + \frac{a_1 c_2}{2} \right) S_3 \quad (\text{C10})$$

$$(\text{C11})$$

$$x_8 = -\frac{\pi\beta_L}{1+R_{21}} \left(\frac{c_2^2 - c_1^2}{2} - 2c_1c_2 \right) - \frac{\pi\beta_L}{1+R_{21}} \left(\frac{3c_1^2 + c_2^2}{2} \right) C_4 \quad (C12)$$

$$y_8 = -\frac{\pi\beta_L}{1+R_{21}} \left(\frac{-3c_1^2 + 2c_1c_2 + c_2^2}{2} \right) S_4 \quad (C13)$$

$$x_1 = \left(\frac{b_1 + b_2}{2} + \frac{\pi\beta_L}{1+R_{21}} \frac{a_1b_1 + a_2b_2}{4} \right) C_{1/2} - \frac{\pi\beta_L}{1+R_{21}} \left(\frac{a_1b_2 + a_2b_1}{4} \right) C_{3/2} \quad (C14)$$

$$y_1 = \left(\frac{b_2 - b_1}{2} + \frac{\pi\beta_L}{1+R_{21}} \frac{a_2b_2 - a_1b_1}{4} \right) S_{1/2} - \frac{\pi\beta_L}{1+R_{21}} \left(\frac{a_2b_1 - a_1b_2}{4} \right) S_{3/2} \quad (C15)$$

$$x_3 = \frac{\pi\beta_L}{1+R_{21}} \left[\left(\frac{3a_1b_2 + 3a_2b_1}{4} \right) C_{1/2} - \left(\frac{3a_1b_1 - 5b_1c_1 + 2b_1c_2 + 3a_2b_2 - 2b_2c_1 - b_2c_2}{4} \right) C_{3/2} \right. \\ \left. - \left(\frac{-2b_2c_2 + 2b_1c_1 + b_1c_2 + 5b_2c_1}{4} \right) C_{5/2} \right] \quad (C16)$$

$$y_3 = -\frac{\pi\beta_L}{1+R_{21}} \left[\left(\frac{3(a_1b_2 - a_2b_1)}{4} \right) S_{1/2} + \left(\frac{-3a_1b_1 + 5b_1c_1 - 2b_1c_2 + 3a_2b_2 - 2b_2c_1 - b_2c_2}{4} \right) S_{3/2} \right. \\ \left. + \left(\frac{2b_2c_2 + 2b_1c_1 + b_1c_2 - 5b_2c_1}{4} \right) S_{5/2} \right] \quad (C17)$$

$$x_5 = -\frac{\pi\beta_L}{1+R_{21}} \left[\left(\frac{-7b_2c_1 + 2b_2c_2 - 2b_1c_1 - 3b_1c_2}{4} \right) C_{3/2} + \left(\frac{7b_1c_1 - 2b_1c_2 + 2b_2c_1 + 3b_2c_2}{4} \right) C_{5/2} \right] \quad (C18)$$

$$y_5 = -\frac{\pi\beta_L}{1+R_{21}} \left[\left(\frac{7b_2c_1 - 2b_2c_2 - 2b_1c_1 - 3b_1c_2}{4} \right) S_{3/2} + \left(\frac{-7b_1c_1 + 2b_1c_2 + 2b_2c_1 + 3b_2c_2}{4} \right) S_{5/2} \right] \quad (C19)$$

These are complicated expressions, but we can gain insight about the effects of asymmetry on the dc and ac response of the SQUID. Firstly, we notice that the harmonics entering the effective supercurrent are the same as those in the symmetric case, except here we have both cosine and sine terms. For $\hat{\Phi} = 0$, we have $y_1 = \dots = y_8 = 0$ so that only the sine terms contribute to the zero-field SQUID response. Interestingly, higher harmonics (e.g. $\sin(2\phi_A)$) contribute to the effective supercurrent at zero-field as opposed to the symmetric case where higher harmonic contributions only affect the SQUID response at nonzero magnetic flux.

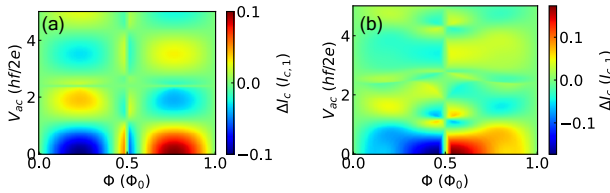


FIG. 7. AC power dependence of ΔI_c for trivial SQUID with (a) $\frac{\beta_L}{1+R_{21}} = 0$ and (b) $\frac{\beta_L}{1+R_{21}} = 0.125$.

1. Voltage-bias solution

As before, we can consider a voltage bias

$$V(\tau) = V_0 + V_1 \cos(\omega\tau) \quad (C20)$$

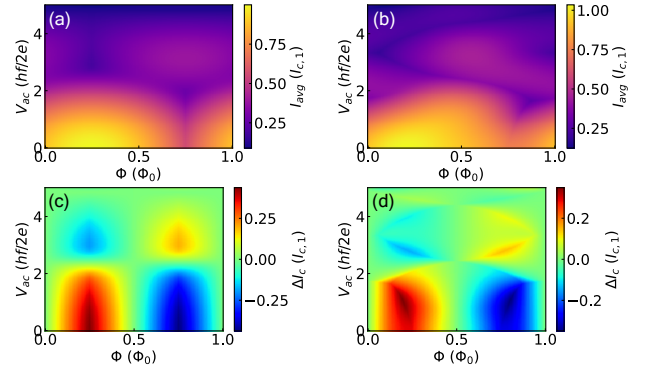


FIG. 8. AC power dependence of I_{avg} and ΔI_c for $2\pi-4\pi$ SQUID with (a) $\frac{\beta_L}{1+R_{21}} = 0$ and (b) $\frac{\beta_L}{1+R_{21}} = 0.125$.

and make use of the ac Josephson effect

$$\frac{d\phi_A}{dt} = \frac{2e}{\hbar} V \quad (C21)$$

to solve for $\phi_A(\tau)$. Then we can use the Jacobi-Anger expansion,

$$e^{iz \sin(\theta)} = \sum_{n=-\infty}^{+\infty} J_n(z) e^{in\theta}, \quad (C22)$$

where J_n are n^{th} order Bessel functions, to calculate the Shapiro steps and each step's width.

We can integrate to solve for $\phi_A(\tau)$:

$$\phi_A(\tau) = \phi_0 + \omega_0\tau + z \sin(\omega\tau) \quad (C23)$$

where ϕ_0 is an arbitrary integration constant, $z = 2eV_1/\hbar\omega$, and $\omega_0 = 2eV_0/\hbar$. Then we have

$$\begin{aligned} \bar{I}_s(\phi_0, \omega_0 = m\omega) = & \sum_n (-1)^n [x_2 \sin(\phi_0) J_n(z) \delta_{m,n} + x_4 \sin(2\phi_0) J_n(2z) \delta_{2m,n} \\ & + x_6 \sin(3\phi_0) J_n(3z) \delta_{3m,n} + x_8 \sin(4\phi_0) J_n(4z) \delta_{4m,n} + x_1 \sin(\phi_0/2) J_n(z/2) \delta_{m/2,n} \\ & + x_3 \sin(3\phi_0/2) J_n(3z/2) \delta_{3m/2,n} + x_5 \sin(5\phi_0/2) J_n(5z/2) \delta_{5m/2,n} + y_2 \cos(\phi_0) J_n(z) \delta_{m,n} \\ & + y_4 \cos(2\phi_0) J_n(2z) \delta_{2m,n} + y_6 \cos(3\phi_0) J_n(3z) \delta_{3m,n} + y_8 \cos(4\phi_0) J_n(4z) \delta_{4m,n} \\ & + y_1 \cos(\phi_0/2) J_n(z/2) \delta_{m/2,n} + y_3 \cos(3\phi_0/2) J_n(3z/2) \delta_{3m/2,n} \\ & + y_5 \cos(5\phi_0/2) J_n(5z/2) \delta_{5m/2,n}] \end{aligned} \quad (\text{C24})$$

Appendix D: Additional Data

Figures 5 and 6 show calculations of the average critical current and critical current difference corresponding to data in Fig. 1(d-h). Figures 7 and 8 show the critical current difference corresponding to data in Fig. 3 and 4, respectively.

* jjcuozz@sandia.gov

- ¹ M A Silaev, A Yu Aladyshkin, M V Silaeva, and A S Aladyshkina, “The diode effect induced by domain-wall superconductivity,” *Journal of Physics: Condensed Matter* **26**, 095702 (2014).
- ² Ryohei Wakatsuki, Yu Saito, Shintaro Hoshino, Yuki M. Itahashi, Toshiya Ideue, Motohiko Ezawa, Yoshihiro Iwasa, and Naoto Nagaosa, “Nonreciprocal charge transport in noncentrosymmetric superconductors,” *Science Advances* **3**, e1602390 (2017), <https://www.science.org/doi/pdf/10.1126/sciadv.1602390>.
- ³ Kenji Yasuda, Hironori Yasuda, Tian Liang, Ryutaro Yoshimi, Atsushi Tsukazaki, Kei S. Takahashi, Naoto Nagaosa, Masashi Kawasaki, and Yoshinori Tokura, “Nonreciprocal charge transport at topological insulator/superconductor interface,” *Nature Communications* **10**, 2734 (2019).
- ⁴ Fuyuki Ando, Yuta Miyasaka, Tian Li, Jun Ishizuka, Tomonori Arakawa, Yoichi Shiota, Takahiro Moriyama, Youichi Yanase, and Teruo Ono, “Observation of superconducting diode effect,” *Nature* **584**, 373–376 (2020).
- ⁵ Jeacheol Shin, Suhan Son, Jonginn Yun, Giung Park, Kaixuan Zhang, Young Jae Shin, Je-Geun Park, and Dohun Kim, “Magnetic proximity-induced superconducting diode effect and infinite magnetoresistance in van der waals heterostructure,” *arXiv*, 2111.05627 (2021).
- ⁶ Yang-Yang Lyu, Ji Jiang, Yong-Lei Wang, Zhi-Li Xiao, Sining Dong, Qing-Hu Chen, Milorad V. Milošević, Huabing Wang, Ralu Divan, John E. Pearson, Peiheng Wu, Francois M. Peeters, and Wai-Kwong Kwok, “Superconducting diode effect via conformal-mapped nanoholes,” *Nature Communications* **12**, 2703 (2021).
- ⁷ Akito Daido, Yuhei Ikeda, and Youichi Yanase, “Intrinsic superconducting diode effect,” *Phys. Rev. Lett.* **128**,

037001 (2022).

- ⁸ Noah F. Q. Yuan and Liang Fu, “Supercurrent diode effect and finite-momentum superconductors,” *Proceedings of the National Academy of Sciences* **119**, e2119548119 (2022), <https://www.pnas.org/doi/pdf/10.1073/pnas.2119548119>.
- ⁹ S. Ilić and F. S. Bergeret, “Theory of the supercurrent diode effect in rashba superconductors with arbitrary disorder,” *Phys. Rev. Lett.* **128**, 177001 (2022).
- ¹⁰ Henry F. Legg, Daniel Loss, and Jelena Klinovaja, “Superconducting diode effect due to magnetochiral anisotropy in topological insulators and rashba nanowires,” *Phys. Rev. B* **106**, 104501 (2022).
- ¹¹ Dhavala Suri, Akashdeep Kamra, Thomas N. G. Meier, Matthias Kronseder, Wolfgang Belzig, Christian H. Back, and Christoph Strunk, “Non-reciprocity of vortex-limited critical current in conventional superconducting microbridges,” *Applied Physics Letters* **121**, 102601 (2022), <https://doi.org/10.1063/5.0109753>.
- ¹² James Jun He, Yukio Tanaka, and Naoto Nagaosa, “A phenomenological theory of superconductor diodes,” *New Journal of Physics* **24**, 053014 (2022).
- ¹³ T. Karabassov, I. V. Bobkova, A. A. Golubov, and A. S. Vasenko, “Hybrid helical state and superconducting diode effect in superconductor/ferromagnet/topological insulator heterostructures,” *Phys. Rev. B* **106**, 224509 (2022).
- ¹⁴ Lorenz Bauriedl, Christian Bäuml, Lorenz Fuchs, Christian Baumgartner, Nicolas Paulik, Jonas M. Bauer, Kai-Qiang Lin, John M. Lupton, Takashi Taniguchi, Kenji Watanabe, Christoph Strunk, and Nicola Paradiso, “Supercurrent diode effect and magnetochiral anisotropy in few-layer nbse2,” *Nature Communications* **13**, 4266 (2022).
- ¹⁵ E. Strambini, M. Spies, N. Ligato, S. Ilifá, M. Rouco, Carmen Gonzalez-Orellana, Maxim Ilyn, Celia Rogero, F. S.

- Bergeret, J. S. Moodera, P. Virtanen, T. T. Heikkilä, and F. Giazotto, “Superconducting spintronic tunnel diode,” *Nature Communications* **13**, 2431 (2022).
- ¹⁶ Sara Chahid, Serafim Teknowijoyo, Iris Mowgood, and Armen Gulian, “High-frequency diode effect in superconducting nb_3sn microbridges,” *Phys. Rev. B* **107**, 054506 (2023).
- ¹⁷ Jiangping Hu, Congjun Wu, and Xi Dai, “Proposed design of a josephson diode,” *Phys. Rev. Lett.* **99**, 067004 (2007).
- ¹⁸ Xiaoyan Shi, Wenlong Yu, Zhigang Jiang, B. Andrei Bernevig, W. Pan, S. D. Hawkins, and J. F. Klem, “Giant supercurrent states in a superconductor-inas/gas-superconductor junction,” *Journal of Applied Physics* **118**, 133905 (2015), <https://doi.org/10.1063/1.4932644>.
- ¹⁹ E. Bocquillon and *et al.*, “Gapless Andreev bound states in the quantum spin Hall insulator HgTe,” *Nature Nanotech* **12**, 137–143 (2017).
- ²⁰ Subhajit Pal and Colin Benjamin, “Quantized josephson phase battery,” *Europhysics Letters* **126**, 57002 (2019).
- ²¹ Kou Misaki and Naoto Nagaosa, “Theory of the nonreciprocal josephson effect,” *Phys. Rev. B* **103**, 245302 (2021).
- ²² C Baumgartner, L Fuchs, A Costa, Jordi Picó-Cortés, S Reinhardt, S Gronin, G C Gardner, T Lindemann, M J Manfra, P E Faria Junior, D Kochan, J Fabian, N Paradiso, and C Strunk, “Effect of rashba and dreselhaus spin-orbit coupling on supercurrent rectification and magnetochiral anisotropy of ballistic josephson junctions,” *Journal of Physics: Condensed Matter* **34**, 154005 (2022).
- ²³ Christian Baumgartner, Lorenz Fuchs, Andreas Costa, Simon Reinhardt, Sergei Gronin, Geoffrey C. Gardner, Tyler Lindemann, Michael J. Manfra, Paulo E. Faria Junior, Denis Kochan, Jaroslav Fabian, Nicola Paradiso, and Christoph Strunk, “Supercurrent rectification and magnetochiral effects in symmetric josephson junctions,” *Nature Nanotechnology* **17**, 39–44 (2022).
- ²⁴ Kun-Rok Jeon, Jae-Keun Kim, Jiho Yoon, Jae-Chun Jeon, Hyeon Han, Audrey Cottet, Takis Kontos, and Stuart S. P. Parkin, “Zero-field polarity-reversible josephson supercurrent diodes enabled by a proximity-magnetized pt barrier,” *Nature Materials* **21**, 1008–1013 (2022).
- ²⁵ Klaus Halterman, Mohammad Alidoust, Ross Smith, and Spencer Starr, “Supercurrent diode effect, spin torques, and robust zero-energy peak in planar half-metallic trilayers,” *Phys. Rev. B* **105**, 104508 (2022).
- ²⁶ Banabir Pal, Anirban Chakraborty, Pranava K. Sivakumar, Margarita Davydova, Ajesh K. Gopi, Avanindra K. Pandeya, Jonas A. Krieger, Yang Zhang, Mihir Date, Sailing Ju, Noah Yuan, Niels B. M. Schröter, Liang Fu, and Stuart S. P. Parkin, “Josephson diode effect from cooper pair momentum in a topological semimetal,” *Nature Physics* **18**, 1228–1233 (2022).
- ²⁷ Heng Wu, Yaojia Wang, Yuanfeng Xu, Pranava K. Sivakumar, Chris Pasco, Ulderico Filippozzi, Stuart S. P. Parkin, Yu-Jia Zeng, Tyrel McQueen, and Mazhar N. Ali, “The field-free josephson diode in a van der waals heterostructure,” *Nature* **604**, 653–656 (2022).
- ²⁸ T. H. Kikkeler, A. A. Golubov, and F. S. Bergeret, “Field-free anomalous junction and superconducting diode effect in spin-split superconductor/topological insulator junctions,” *Phys. Rev. B* **106**, 214504 (2022).
- ²⁹ Yi Zhang, Yuhao Gu, Pengfei Li, Jiangping Hu, and Kun Jiang, “General theory of josephson diodes,” *Phys. Rev. X* **12**, 041013 (2022).
- ³⁰ Margarita Davydova, Saranesh Prembabu, and Liang Fu, “Universal josephson diode effect,” *Science Advances* **8**, eabo0309 (2022), <https://www.science.org/doi/pdf/10.1126/sciadv.abo0309>.
- ³¹ Stefan Ilić, Pauli Virtanen, Tero T. Heikkilä, and F. Sebastián Bergeret, “Current rectification in junctions with spin-split superconductors,” *Phys. Rev. Appl.* **17**, 034049 (2022).
- ³² Martina Trahms, Larissa Melischek, Jacob F. Steiner, Bharti Mahendru, Idan Tamir, Nils Bogdanoff, Olof Peters, Gaël Reecht, Clemens B. Winkelmann, Felix von Oppen, and Katharina J. Franke, “Diode effect in josephson junctions with a single magnetic atom,” *Nature* **615**, 628–633 (2023).
- ³³ Lars Onsager, “Reciprocal relations in irreversible processes. i.” *Phys. Rev.* **37**, 405–426 (1931).
- ³⁴ Ryogo Kubo, “Statistical-mechanical theory of irreversible processes. i. general theory and simple applications to magnetic and conduction problems,” *Journal of the Physical Society of Japan* **12**, 570–586 (1957), <https://doi.org/10.1143/JPSJ.12.570>.
- ³⁵ G. L. J. A. Rikken, J. Fölling, and P. Wyder, “Electrical magnetochiral anisotropy,” *Phys. Rev. Lett.* **87**, 236602 (2001).
- ³⁶ V. M. Krasnov, V. A. Oboznov, and N. F. Pedersen, “Fluxon dynamics in long josephson junctions in the presence of a temperature gradient or spatial nonuniformity,” *Phys. Rev. B* **55**, 14486–14498 (1997).
- ³⁷ N. Tuitou, P. Bernstein, J. F. Hamet, Ch. Simon, L. Méchin, J. P. Contour, and E. Jacquet, “Nonsymmetric current-voltage characteristics in ferromagnet/superconductor thin film structures,” *Applied Physics Letters* **85**, 1742–1744 (2004), <https://doi.org/10.1063/1.1789231>.
- ³⁸ D. Y. Vodolazov, B. A. Gribkov, S. A. Gusev, A. Yu. Klimov, Yu. N. Nozdrin, V. V. Rogov, and S. N. Vdovichev, “Considerable enhancement of the critical current in a superconducting film by a magnetized magnetic strip,” *Phys. Rev. B* **72**, 064509 (2005).
- ³⁹ A. Papon, K. Senapati, and Z. H. Barber, “Asymmetric critical current of niobium microbridges with ferromagnetic stripe,” *Applied Physics Letters* **93**, 172507 (2008), <https://doi.org/10.1063/1.3009207>.
- ⁴⁰ G. Carapella, P. Sabatino, and G. Costabile, “Asymmetry, bistability, and vortex dynamics in a finite-geometry ferromagnet-superconductor bilayer structure,” *Phys. Rev. B* **81**, 054503 (2010).
- ⁴¹ Taras Golod and Vladimir M. Krasnov, “Demonstration of a superconducting diode-with-memory, operational at zero magnetic field with switchable nonreciprocity,” *Nature Communications* **13**, 3658 (2022).
- ⁴² A. Yu Kitaev, “Fault-tolerant quantum computation by anyons,” *Annals of Physics* (2003), 10.1016/S0003-4916(02)00018-0, arXiv:9707021 [quant-ph].
- ⁴³ H.-J. Kwon, K Sengupta, and V M Yakovenko, “Fractional ac Josephson effect in p- and d-wave superconductors,” *The European Physical Journal B - Condensed Matter and Complex Systems* **37**, 349–361 (2004).
- ⁴⁴ Chetan Nayak, Steven H. Simon, Ady Stern, Michael Freedman, and Sankar Das Sarma, “Non-Abelian anyons and topological quantum computation,” *Reviews of Modern Physics* (2008), 10.1103/RevModPhys.80.1083, arXiv:0707.1889.

- ⁴⁵ Liang Fu and C. L. Kane, “Josephson current and noise at a superconductor/quantum-spin-Hall-insulator/superconductor junction,” *Phys. Rev. B* **79**, 161408 (2009).
- ⁴⁶ Jay D. Sau, Roman M. Lutchyn, Sumanta Tewari, and S. Das Sarma, “Generic new platform for topological quantum computation using semiconductor heterostructures,” *Phys. Rev. Lett.* **104**, 040502 (2010).
- ⁴⁷ Jason Alicea, “New directions in the pursuit of majorana fermions in solid state systems,” *Reports on Progress in Physics* **75**, 076501 (2012).
- ⁴⁸ Falko Pientka, Anna Keselman, Erez Berg, Amir Yacoby, Ady Stern, and Bertrand I. Halperin, “Topological superconductivity in a planar Josephson junction,” *Physical Review X* (2017), 10.1103/PhysRevX.7.021032, arXiv:1609.09482.
- ⁴⁹ Michael Hell, Martin Leijnse, and Karsten Flensberg, “Two-dimensional platform for networks of majorana bound states,” *Phys. Rev. Lett.* **118**, 107701 (2017).
- ⁵⁰ David Aasen, Michael Hell, Ryan V. Mishmash, Andrew Higginbotham, Jeroen Danon, Martin Leijnse, Thomas S. Jespersen, Joshua A. Folk, Charles M. Marcus, Karsten Flensberg, and Jason Alicea, “Milestones toward Majorana-based quantum computing,” *Phys. Rev. X* **6**, 031016 (2016).
- ⁵¹ Eduardo J. H. Lee, Xiaocheng Jiang, Ramón Aguado, Georgios Katsaros, Charles M. Lieber, and Silvano De Franceschi, “Zero-bias anomaly in a nanowire quantum dot coupled to superconductors,” *Phys. Rev. Lett.* **109**, 186802 (2012).
- ⁵² G. Kells, D. Meidan, and P. W. Brouwer, “Near-zero-energy end states in topologically trivial spin-orbit coupled superconducting nanowires with a smooth confinement,” *Phys. Rev. B* **86**, 100503 (2012).
- ⁵³ Jorge Cayao, Elsa Prada, Pablo San-Jose, and Ramón Aguado, “Sns junctions in nanowires with spin-orbit coupling: Role of confinement and helicity on the subgap spectrum,” *Phys. Rev. B* **91**, 024514 (2015).
- ⁵⁴ Christopher Reeg, Olesia Dmytruk, Denis Chevallier, Daniel Loss, and Jelena Klinovaja, “Zero-energy andreev bound states from quantum dots in proximitized rashba nanowires,” *Phys. Rev. B* **98**, 245407 (2018).
- ⁵⁵ Fernando Peñaranda, Ramón Aguado, Pablo San-Jose, and Elsa Prada, “Quantifying wave-function overlaps in inhomogeneous majorana nanowires,” *Phys. Rev. B* **98**, 235406 (2018).
- ⁵⁶ Adriaan Vuik, Bas Nijholt, Anton R. Akhmerov, and Michael Wimmer, “Reproducing topological properties with quasi-Majorana states,” *SciPost Phys.* **7**, 061 (2019).
- ⁵⁷ Chun-Xiao Liu, Jay D. Sau, Tudor D. Stanescu, and S. Das Sarma, “Conductance smearing and anisotropic suppression of induced superconductivity in a majorana nanowire,” *Phys. Rev. B* **99**, 024510 (2019).
- ⁵⁸ J. Chen, B. D. Woods, P. Yu, M. Hocevar, D. Car, S. R. Plissard, E. P. A. M. Bakkers, T. D. Stanescu, and S. M. Frolov, “Ubiquitous non-majorana zero-bias conductance peaks in nanowire devices,” *Phys. Rev. Lett.* **123**, 107703 (2019).
- ⁵⁹ Oladunjoye A. Awoga, Jorge Cayao, and Annica M. Black-Schaffer, “Supercurrent detection of topologically trivial zero-energy states in nanowire junctions,” *Phys. Rev. Lett.* **123**, 117001 (2019).
- ⁶⁰ Benjamin D. Woods, Jun Chen, Sergey M. Frolov, and Tudor D. Stanescu, “Zero-energy pinning of topologically trivial bound states in multiband semiconductor-superconductor nanowires,” *Phys. Rev. B* **100**, 125407 (2019).
- ⁶¹ Elsa Prada, Pablo San-Jose, Michiel W. A. de Moor, Attila Geresdi, Eduardo J. H. Lee, Jelena Klinovaja, Daniel Loss, Jesper Nygård, Ramón Aguado, and Leo P. Kouwenhoven, “From andreev to majorana bound states in hybrid superconductor–semiconductor nanowires,” *Nature Reviews Physics* **2**, 575–594 (2020).
- ⁶² Marco Valentini, Fernando Peñaranda, Andrea Hofmann, Matthias Brauns, Robert Hauschild, Peter Krogstrup, Pablo San-Jose, Elsa Prada, Ramón Aguado, and Georgios Katsaros, “Nontopological zero-bias peaks in full-shell nanowires induced by flux-tunable andreev states,” *Science* **373**, 82–88 (2021), <https://www.science.org/doi/pdf/10.1126/science.abf1513>.
- ⁶³ Richard Hess, Henry F. Legg, Daniel Loss, and Jelena Klinovaja, “Local and nonlocal quantum transport due to andreev bound states in finite rashba nanowires with superconducting and normal sections,” *Phys. Rev. B* **104**, 075405 (2021).
- ⁶⁴ Matthieu C. Dartiailh, William Mayer, Joseph Yuan, Kaushini S. Wickramasinghe, Alex Matos-Abiague, Igor Žutić, and Javad Shabani, “Phase Signature of Topological Transition in Josephson Junctions,” *Physical Review Letters* **126**, 036802 (2021).
- ⁶⁵ Morteza Aghaee and et. al, “InAs-Al Hybrid Devices Passing the Topological Gap Protocol,” *arXiv* , 2207.02472 (2022).
- ⁶⁶ Leonid P. Rokhinson, Xinyu Liu, and Jacek K. Furdyna, “The fractional a.c. Josephson effect in a semiconductor–superconductor nanowire as a signature of Majorana particles,” *Nature Physics* **8**, 795–799 (2012).
- ⁶⁷ J. Wiedenmann, E. Bocquillon, R. S. Deacon, S. Hartinger, O. Herrmann, T. M. Klapwijk, L. Maier, C. Ames, C. Brüne, C. Gould, A. Oiwa, K. Ishibashi, S. Tarucha, H. Buhmann, and L. W. Molenkamp, “ 4ϕ -periodic Josephson supercurrent in HgTe-based topological Josephson junctions,” *Nature Communications* (2016), 10.1038/ncomms10303, arXiv:1503.05591.
- ⁶⁸ W. Yu, W. Pan, D. L. Medlin, M. A. Rodriguez, S. R. Lee, Zhi Qiang Bao, and F. Zhang, “ π and 4π Josephson Effects Mediated by a Dirac Semimetal,” *Physical Review Letters* (2018), 10.1103/PhysRevLett.120.177704.
- ⁶⁹ Dong-Xia Qu, Joseph J. Cuozzo, Nick E. Teslich, Keith G. Ray, Zurong Dai, Tian T. Li, George F. Chapline, Jonathan L. DuBois, and Enrico Rossi, “Phase-Slip Lines and Anomalous Josephson Effects in a Tungsten Clusters-Topological Insulator Microbridge,” (2022), arXiv:2301.00086 [cond-mat].
- ⁷⁰ Matthieu C. Dartiailh, Joseph J. Cuozzo, Bassel H. Elfeky, William Mayer, Joseph Yuan, Kaushini S. Wickramasinghe, Enrico Rossi, and Javad Shabani, “Missing Shapiro steps in topologically trivial Josephson junction on InAs quantum well,” *Nature Communications* (2021), 10.1038/s41467-020-20382-y, arXiv:2005.00077.
- ⁷¹ A. A. Kopasov, A. G. Kutlin, and A. S. Mel’nikov, “Geometry controlled superconducting diode and anomalous josephson effect triggered by the topological phase transition in curved proximitized nanowires,” *Phys. Rev. B* **103**, 144520 (2021).
- ⁷² Henry F. Legg, Katharina Laubscher, Daniel Loss, and Jelena Klinovaja, “Parity protected superconducting diode effect in topological Josephson junctions,” *arXiv* ,

- 2301.13740 (2023).
- ⁷³ T. A. Fulton, L. N. Dunkleberger, and R. C. Dynes, “Quantum interference properties of double Josephson junctions,” *Phys. Rev. B* **6**, 855–875 (1972).
- ⁷⁴ Ya. V. Fominov and D. S. Mikhailov, “Asymmetric higher-harmonic SQUID as a Josephson diode,” *Phys. Rev. B* **106**, 134514 (2022).
- ⁷⁵ Rubén Seoane Souto, Martin Leijnse, and Constantin Schrader, “Josephson diode effect in supercurrent interferometers,” *Phys. Rev. Lett.* **129**, 267702 (2022).
- ⁷⁶ B. Van Heck, F. Hassler, A. R. Akhmerov, and C. W.J. Beenakker, “Coulomb stability of the 4π -periodic Josephson effect of Majorana fermions,” *Physical Review B - Condensed Matter and Materials Physics* (2011), 10.1103/PhysRevB.84.180502, arXiv:1108.1095.
- ⁷⁷ Michael Hell, Martin Leijnse, and Karsten Flensberg, “Two-Dimensional Platform for Networks of Majorana Bound States,” *Phys. Rev. Lett.* **118**, 107701 (2017).
- ⁷⁸ R. A. Snyder, C. J. Trimble, C. C. Rong, P. A. Folkes, P. J. Taylor, and J. R. Williams, “Weak-link Josephson Junctions Made from Topological Crystalline Insulators,” *Physical Review Letters* (2018), 10.1103/PhysRevLett.121.097701, arXiv:1710.06077.
- ⁷⁹ Gil Ho Lee, Sol Kim, Seung Hoon Jhi, and Hu Jong Lee, “Ultimately short ballistic vertical graphene Josephson junctions,” *Nature Communications* (2015), 10.1038/ncomms7181.
- ⁸⁰ R. Pangotra, B. Raes, Clécio C. de Souza Silva, I. Cools, W. Keijers, J. E. Scheerder, V. V. Moshchalkov, and J. Van de Vondel, “Giant fractional Shapiro steps in anisotropic Josephson junction arrays,” *Communications Physics* (2020), 10.1038/s42005-020-0315-5.
- ⁸¹ F. Romeo and R. De Luca, “Shapiro steps in symmetric π -SQUID’s,” *Physica C: Superconductivity and its Applications* (2005), 10.1016/j.physc.2005.02.011.
- ⁸² x_m and y_m are defined explicitly in Appendix C.
- ⁸³ M. Veldhorst, C. G. Molenaar, C. J.M. Verwijs, H. Hilgenkamp, and A. Brinkman, “Optimizing the Majorana character of SQUIDs with topologically nontrivial barriers,” *Physical Review B - Condensed Matter and Materials Physics* (2012), 10.1103/PhysRevB.86.024509.
- ⁸⁴ In terms of physical parameters, we can take $I_{c,1} = 0.5 \mu\text{A}$ and $R_{n,1} = 85 \Omega$ ($E_{J,1} = 2eI_{c,1}R_{n,1} = 85 \mu\text{eV}$) at driving frequencies 2, 7 and 12 GHz.
- ⁸⁵ Carlo Ciaccia, Roy Haller, Asbjørn C. C. Drachmann, Tyler Lindemann, Michael J. Manfra, Constantin Schrader, and Christian Schönenberger, “Gate-tunable Josephson diode in proximitized inas supercurrent interferometers,” *Phys. Rev. Res.* **5**, 033131 (2023).
- ⁸⁶ Axel Leblanc, Chotivut Tangchingchai, Zahra Sadre Montaz, Elyjah Kiyooka, Jean-Michel Hartmann, Gonzalo Troncoso Fernandez-Bada, Boris Brun-Barriere, Vivien Schmitt, Simon Zihlmann, Romain Maurand, Etienne Dumur, Silvano De Franceschi, and Francois Lefloch, “From nonreciprocal to charge-4e supercurrents in Ge-based Josephson devices with tunable harmonic content,” *arXiv* , 2311.15371 (2023).